Journal of Alloys and Compounds 565 (2013) 37–43

Contents lists available at SciVerse ScienceDirect

Journal of Alloys and Compounds

journal homepage: www.elsevier.com/locate/jalcom

Annealing effect on hydrogen storage property of Co-free $La_{1.8}Ti_{0.2}MgNi_{8.7}Al_{0.3}$ alloy

Weiqing Jiang *, Changsheng Qin, Rongrong Zhu, Jin Guo *

College of Physics Science and Technology, Key Laboratory of National Education Ministry for Nonferrous Metals and Materials Processing Technology, Guangxi University, Nanning 530004, China

ARTICLE INFO

Article history:
Received 26 November 2012
Received in revised form 23 February 2013
Accepted 26 February 2013
Available online 14 March 2013

Keywords:
La–Mg–Ni-based alloy
Annealing treatment
Hydrogen storage property
Electrochemical characteristic

ABSTRACT

A series of Co-free $La_{1.8}Ti_{0.2}MgNi_{8.7}Al_{0.3}$ alloys are prepared by magnetic levitation melting followed by annealing treatment. The hydrogen storage properties of as-cast and annealed $La_{1.8}Ti_{0.2}MgNi_{8.7}Al_{0.3}$ alloys are investigated systematically. The results show that $La(Ni,Al)_5$ and $LaMg_2Ni_9$ are the main phases and a $LaNi_2$ phase disappears at 900 °C. The enthalpies of the experimental alloys are close to −30.6 kJ/mol H_2 of $LaNi_5$ compound. Comparing with as-cast alloy, annealed alloys exhibit larger hydrogen storage capacity, lower hydrogen absorption/desorption plateau pressure and longer cycle life. At 60% discharge capacity retention, the maximum charge–discharge cycles, 205 cycles (annealed 900 °C), are two times the minimum, 102 cycles (as-cast). The positive impact of annealing on the charge transfer rate at surface and the hydrogen diffusion rate in bulk enhances the high rate dischargeability. Annealed alloy (900 °C) shows good overall hydrogen storage properties.

1. Introduction

With the rapid development of electric equipments, the demand for the nickel/metal-hydride (Ni/MH) rechargeable batteries with higher performances has increased fast. This requires the hydrogen storage alloys, which are used as the negative electrode material of Ni/MH battery, to possess higher energy density, faster activation, better rate capability and lower cost [1,2].

Recently, $AB_{3\text{-}3.8}$-type La–Mg–Ni-based alloys have become attractive metal hydride electrode materials due to their large hydrogen storage capacity and good electrochemical properties [3–6]. Considerable investigations on La–Mg–Ni system are devoted to develop low-cost alloys with good electrochemical performances in order to satisfy the requirements for Ni/MH batteries [1,2]. It is well known that Co is a key element for suppressing capacity degradation in AB_5-type alloys [7,8]. But many studies revealed that the impact of Co on the cycling stability in $AB_{3\text{-}3.8}$-type alloys is not so much important as that in AB_5-type alloys [9,10]. Meanwhile, Co element is not only unfriendly to the environment, but also increases the cost of the batteries. Developing low-Co or Co-free hydrogen storage alloys is important and necessary [2,11–13]. Furthermore, it is found that annealing can make a positive contribution to hydrogen storage properties, such as hydrogen storage capacity, discharge capacity and cycling life [14–17]. Sakai et al. [14] investigated the rare-earth-based hydrogen storage alloys, and revealed that annealing could decrease crystal defects and increase composition homogenization, and consequently enhance the discharge capacity and cyclic stability of the alloys. Pan et al. studied the La–Mg–Ni–Co system hydrogen storage alloys, and reported that annealing significantly prolonged the cycle life of $La_{0.67}Mg_{0.33}Ni_{2.5}Co_{0.5}$ [15] and $La_{0.7}Mg_{0.3}Ni_{2.45}Co_{0.75}Mn_{0.1}Al_{0.2}$ [16] alloy electrodes due to composition homogenization. Moreover, we have compared the Co-free $La_{2-x}Ti_xMgNi_9$ (x = 0.2, 0.3) alloys with and without annealing treatment [17], and found that $La_{1.8}Ti_{0.2}MgNi_9$ alloy annealed at 900 °C showed the best overall properties, but its cyclic stability was required to further improved. To enhance the electrochemical properties of $La_{1.8}Ti_{0.2}MgNi_9$ alloy and make it much more suitable for practical application, in this study, Al substitution for Ni is applied to prepare $La_{1.8}Ti_{0.2}MgNi_{8.7}Al_{0.3}$ alloy, since Al is believed to form a porous oxide layer on the alloy surface during charge/discharge cycling, protecting La–Mg–Ni-based hydride material from further corrosion in KOH electrolyte [18]. Then, $La_{1.8}Ti_{0.2}MgNi_{8.7}Al_{0.3}$ alloy is applied annealing treatment, and the annealing effect on the hydrogen storage properties of the alloy is studied in detail.

2. Experimental

$La_{1.8}Ti_{0.2}MgNi_{8.7}Al_{0.3}$ alloy was prepared by magnetic levitation melting under Ar atmosphere. Some ingot alloys were annealed at 800 °C or 900 °C for 10 h under vacuum. The purity of all metals (La, Ti, Mg, Ni, Al) is above 99.9%.

The crystal structures of each sample were examined by X-ray powder diffraction (XRD) with Cu Kα radiation. The lattice parameters and cell volumes were analyzed by the Materials Data Inc. software Jade 5.0 and a Powder Diffraction File (PDF release 2002). The morphology and composition of the alloy were determined by scanning

* Corresponding author. Tel./fax: +86 771 3237386.
E-mail addresses: wqjiang@gxu.edu.cn (W. Jiang), guojin@gxu.edu.cn (J. Guo).

0925-8388/$ - see front matter © 2013 Elsevier B.V. All rights reserved.
http://dx.doi.org/10.1016/j.jallcom.2013.02.178

electron microscopy (SEM) coupled with energy dispersive spectrometer (EDS). The hydrogen absorption/desorption behavior was studied with the help of Seiverts-type apparatus in the temperature range 30–70 °C and the pressure range 20–0.06 atm.

The hydride electrodes were prepared by cold pressing alloy powder (200 mesh) with carbonyl nickel powder in a weight ratio of 1:4 under 25 MPa pressure. The electrochemical properties were performed in a standard three electrode cell, consisting of a metal hydride electrode, a $Ni(OH)_2$/NiOOH counter electrode, and a Hg/HgO reference electrode with 6 mol/L KOH as the electrolyte. Charge–discharge tests were carried out on DC-5 automatic battery testing instrument at charge rate 100 mA/g, discharge rate 80 mA/g and cut-off potential −0.5 V (vs. Hg/HgO electrode). High rate dischargeability (HRD) was done at different discharge current densities using Arbin automatic instrument. Electrochemical impedance spectroscopy (EIS) was conducted at 50% depth of discharge (DOD) under open circuit condition using Gamry automatic instrument with frequency range 10 kHz to 5 mHz and AC voltage 5 mV. The linear polarization and Tafel polarization were produced on Gamry automatic instrument at 50% DOD by scanning electrode potential at a rate 0.1 mV/s from −5 mV to 5 mV (vs. open circuit potential) and 10 mV/s from −0.3 V to 1 V (vs. open circuit potential), respectively. The cyclic voltammetry was measured on Gamry automatic instrument at scanning rate 5 mV/s from −1.2 V to 0 V (vs. Hg/HgO electrode). The hydrogen diffusion coefficient was estimated by potentiostatic discharge and the experiment was carried out on Gamry automatic instrument at fully charged state with constant potential +600 mV for 4800 s. All the electrochemical tests mentioned above were measured at room temperature after the alloy electrodes were fully activated.

3. Results and discussion

3.1. Microstructure

Fig. 1a shows the XRD patterns of as-cast and annealed $La_{1.8}Ti_{0.2}MgNi_{8.7}Al_{0.3}$ alloys and Table 1 lists the lattice parameters obtained from XRD analysis. It can be seen from Fig. 1a and Table 1 that the experimental alloys all contain two major phases, $La(Ni,Al)_5$ phase ($CaCu_5$-type; space group P6/mmm) and $LaMg_2Ni_9$ phase ($PuNi_3$-type; space group R3m). $LaNi_2$ phase ($MgCu_2$-type; space group Fd-3m) disappears at 900 °C. After annealing, most main peaks corresponding to $La(Ni,Al)_5$ or $LaMg_2Ni_9$ phases shift to smaller diffraction angles, and become narrower and sharper, as illustrated by the amplified diffraction patterns from 29.5° to 43.5°, Fig. 1b. This implies an increased cell volume of $La(Ni,Al)_5$ or $LaMg_2Ni_9$ phases [10,19] (Table 1) and good composition homogenization [20,21], respectively.

Fig. 2a presents the SEM image of annealed alloy (900 °C) as a representative example $La_{1.8}Ti_{0.2}MgNi_{8.7}Al_{0.3}$ alloys. The phase compositions determined by EDS analysis, Fig. 2b and c, are La(Ni, Al)$_5$ phase (the dark region marked with A) and $LaMg_2Ni_9$ phase (the grey region marked with B), respectively. This result is in agreement with that of XRD analysis.

3.2. Hydrogen absorption/desorption property

To study the hydrogen absorption/desorption behavior of as-cast and annealed $La_{1.8}Ti_{0.2}MgNi_{8.7}Al_{0.3}$ alloys, pressure–composition isotherms (PCIs) are plotted in Fig. 3. From these curves, the maximum hydrogen storage capacity (the total capacity under 20 atm, M_{max}) and the hydrogen absorption/desorption plateau pressure (the pressure at 50% total capacity, P_{abs}/P_{des}) can be obtained, and the results measured at 30 °C are summarized in Table 2. It is found that with increased annealing temperature, M_{max} obtained in Fig. 3a goes up from 1.21 wt.% (as-cast) to 1.26 wt.% (annealed 800 °C) and 1.31 wt.% (annealed 900 °C). This trend is also evident in Fig. 3b and c. For annealed alloys, the expansion of cell volume providing more sites for hydrogen storage is responsible for the higher hydrogen capacity. In addition, P_{abs}/P_{des} is reduced by heat treatment, e.g., at 30 °C, P_{abs}/P_{des} starts at 0.87/0.28 atm (as-cast), gradually decreases to 0.79/0.23 atm (annealed 800 °C) and 0.69/0.15 atm (annealed 900 °C), respectively. Similar phenomenon can also be observed at testing temperature 50 °C and 70 °C.

Table 1
Lattice parameters of as-cast and annealed $La_{1.8}Ti_{0.2}MgNi_{8.7}Al_{0.3}$ alloys.

Sample	Phase	a (Å)	b (Å)	c (Å)	V (Å^3)
As-cast	$La(Ni,Al)_5$	5.00	5.00	4.00	86.85
	$LaMg_2Ni_9$	4.99	4.99	24.19	521.65
	$LaNi_2$	7.13	7.13	7.13	362.45
Annealed 800 °C	$La(Ni,Al)_5$	5.02	5.02	4.01	87.33
	$LaMg_2Ni_9$	4.99	4.99	24.21	522.68
	$LaNi_2$	7.13	7.13	7.13	362.45
Annealed 900 °C	$La(Ni,Al)_5$	5.02	5.02	4.02	87.47
	$LaMg_2Ni_9$	5.01	5.01	24.29	527.83

The pressure discrepancy between hydrogen absorption and desorption forms a hysteresis loop, which can be characterized by a hysteresis factor, calculated using $H_f = \ln(P_{abs}/P_{des})$, where P_{abs} and P_{des} stand for the hydrogen absorption and desorption plateau pressure, respectively. Table 2 lists the hysteresis factor H_f at 30 °C. As noted in Table 2, H_f becomes larger after annealing, which indicates the reduction of the reversibility between hydrogen absorption and desorption [22], and may be ascribed to the homogeneous composition for decreasing grain boundaries and lattice defects, and subsequently increasing the obstruction in hydrogenation and dehydrogenation process [17,23].

An understanding of hydride thermodynamics is very important for comparing different hydrides. The thermodynamic parameters of metal hydrides, enthalpy change (ΔH) and entropy change (ΔS), can be determined from the slope and the intercept of Van't Hoff plot (Fig. 4) based on Van't Hoff equation $\ln P = \Delta H/RT - \Delta S/R$. The ΔH is calculated to be −36.44, −34.78 and −35.07 kJ/mol H_2, and ΔS is found to be −109.85, −102.67 and −100.09 J/mol H_2 K corresponding to as-cast and annealed alloys at 800 °C and 900 °C, respectively. The ΔH absolute values observed in the

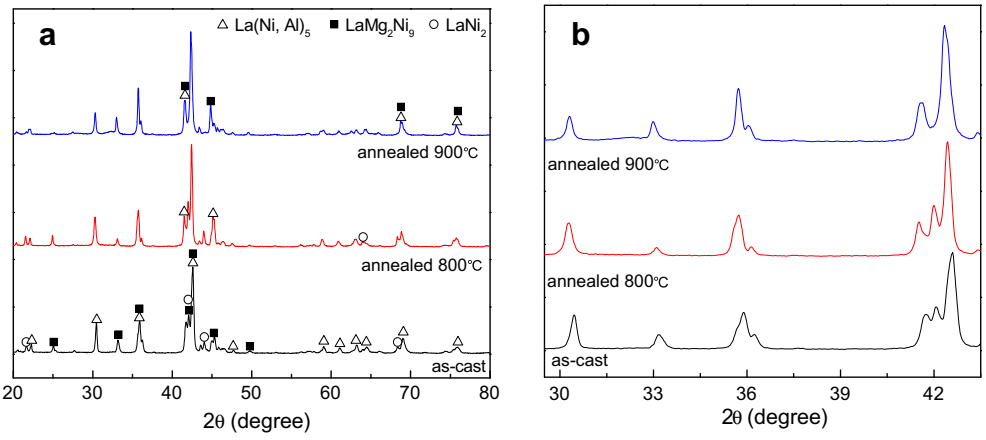

Fig. 1. XRD patterns of as-cast and annealed $La_{1.8}Ti_{0.2}MgNi_{8.7}Al_{0.3}$ alloys (a) and the amplification from 29.5° to 43.5° (b).